ELSEVIER

Coordination Chemistry Reviews 226 (2002) 143–151

COORDINATION CHEMISTRY REVIEWS

www.elsevier.com/locate/ccr

Structures and properties of assembled oxidized metal complexes with $C_8H_4S_8$ and related sulfur-rich dithiolate ligands

G. Matsubayashi *, M. Nakano, H. Tamura

Department of Applied Chemistry, Graduate School of Engineering, Osaka University, 1-16 Machikaneyama, Toyonaka, Osaka 560-0043, Japan

Received 4 April 2001; accepted 17 August 2001

Contents

Abstract

Metal complexes with the $C_8H_4S_8^{2-}$ ligand [2-{(4,5-ethylenedithio)-1,3-dithiole-2-ylidene}-1,3-dithiole-4,5-dithiolate(2 −)] of the types of $[M(C_8H_4S_8)_2]^{n-}$ [M = Pt(II), Au(III); n = 1, 2], $[M(N–N)(C_8H_4S_8)]$ [M = Pd(II), Pt(II); N–N = 2,2′-bipyridine, etc.], $[Sn(C_8H_4S_8)_3]^{2-}$, $[PhSn(C_8H_4S_8)_2]^{-}$, $[M(O)(C_8H_4S_8)_2]^{2-}$ [M = V(IV), Mo(IV)], $[Co(\eta^5\text{-}C_5H_5)(C_8H_4S_8)]$, $[M(L)_2(C_8H_4S_8)]$ [M = Ti(IV), Zr(IV)], $[M(L)(C_8H_4S_8)_2]^{-}$ [M = Ti(IV), Zr(IV), Hf(IV); L = $\eta^5\text{-}C_5H_5$ and $\eta^5\text{-}C_5Me_5$] and $[Fe(\eta^5\text{-}C_5H_5)(CO)_2(L–L)Fe(\eta^5\text{-}C_5H_5)(CO)_2]$ (L = $C_3S_5–C_3S_5$, $C_8H_4S_8–C_8H_4S_8$) and metal complexes with related sulfur-rich dithiolate ligands have been prepared. Their electrochemical and spectroscopic properties have been studied and crystal structures of some complexes clarified. Some of their oxidized species have exhibited high electrical conductivities of $1–10^{-1}$ S cm^{-1} measured for compacted pellets at room temperature. © 2002 Elsevier Science B.V. All rights reserved.

Keywords: Dithiolate complexes; Cyclopentadienyl metal complexes; Oxometallates; Electrical conductivity; Oxidation/reduction; Crystal structures

1. Introduction

Metal complexes with sulfur-rich dithiolate ligands attract much attention, since solids of their oxidized species often become good electrical conductors. Especially, oxidized planar metal complexes of the type $[M(C_3S_5)_2]^{n-}$ [$C_3S_5^{2-}$ = 4,5-disulfanyl-1,3-dithiole-2-thionate(2 −); M = Ni(II), Pd(II), Pt(II) and Au(III); $n < 1$] exhibit high electrical conductivities [1–4], and some Ni(II) and Pd(II) complexes are known as superconductors [4,5]. Effective electron-conduction pathways are formed by molecular interactions through many non-bonded S···S contacts among the C_3S_5 ligand moieties in the solid state.

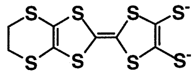

A

Metal complexes with the $C_8H_4S_8^{2-}$ ligand [2-{(4,5-ethylenedithio)-1,3-dithiole-2-ylidene}-1,3-dithiole-4,5-dithiolate(2 −); **A**] as a further extended π-electron system are also expected to afford excellent electrical conductors: since this ligand contains many sulfur

---

* Corresponding author. Tel.: + 81-6-6850-5769; fax: + 81-6-6850-5785.

E-mail address: matsu@ch.wani.osaka-u.ac.jp (G. Matsubayashi).

PII: S0010-8545(01)00423-4

atoms, in various types of the oxidized metal complexes, even in non-planar species, effective molecular interactions via S···S contacts can be formed in the solid state leading to the formation of good electron-conduction pathways. Recently, some metal complexes with sulfur-rich dithiolate ligands having the C_6S_8 skeleton similar to **A** and related ligands also have been studied and their oxidized complexes have often exhibited high electrical conductivities [6–12].

Preparations, structures, spectroscopic and electrochemical properties of various metal complexes with the $C_8H_4S_8$ ligand and with related sulfur-rich dithiolate ligands, together with their oxidation, are described. Electrical conductivities of solids of their oxidized species are also discussed.

2. Planar metal complexes

$[NBu_4][Au(C_8H_4S_8)_2]$ (**1**) [13] and $[NBu_4]_2[Pt(C_8H_4S_8)_2]$ (**2**) [14] were prepared by the reactions of $K[AuCl_4]\cdot 2H_2O$ or K_2PtCl_4 with $Na_2[C_8H_4S_8]$ obtained from $C_8H_4S_8(CH_2C_6H_4OAc\text{-}p)_2$ or $C_8H_4S_8(CH_2CH_2CN)_2$ [14–16]. First oxidation potentials of these complexes are much lower than those of the corresponding C_3S_5-analogs: **1**, $+0.12$ V and **2**, -0.47 V (vs. SCE). Cf. $[NBu_4][Au(C_3S_5)_2]$, $+0.32$ V [17] and $[NBu_4]_2[Pt(C_3S_5)_2]$, -0.08 V (vs. SCE) [18].

Complexes **1** and **2** were oxidized by iodine, $[Fe(\eta^5\text{-}C_5H_5)_2]^+$ or $[Fe(\eta^5\text{-}C_5Me_5)_2]^+$ cation to afford $[NBu_4]_{0.05}[Au(C_8H_4S_8)_2]$, $[NBu_4]_{0.05}[Pt(C_8H_4S_8)_2]$ and $[NBu_4]_{0.1}[Pt(C_8H_4S_8)_2]$, also showing high electrical conductivities of 2.8, 6.9 and 5.5 $S\,cm^{-1}$ [compacted pellets at room temperature (r.t.)], respectively [19]. These oxidized Pt(II) complexes exhibited an EPR signal at $g = 2.01$ due to the paramagnetic moieties with the $C_8H_4S_8$ ligand-centered oxidation. The essentially one-electron oxidized Au(III) complex showed no EPR signal, suggesting an association of the paramagnetic species, as observed for $[Au(S_2C_2S_2C_2H_4)_2]^0$ [20]. The $C_8H_4S_8$ ligand-centered oxidation and planar geometry of these complexes result in an effective molecular interaction through many S···S non-bonded contacts for an electron-conduction pathway. Solids of $Na_{1.5}[Ni(C_8H_4S_8)_2]$ obtained directly by the reaction of $Na_2[C_8H_4S_8]$ with $NiCl_2\cdot 2H_2O$ exhibited an electrical conductivity of 17 $S\,cm^{-1}$ [19].

Table 1
Electrical conductivities ($\sigma_{r.t.}$) [a]

Complex	$\sigma_{r.t.}$ ($S\,cm^{-1}$)
$[Pt(Bu\text{-}pya)(C_8H_4S_8)](I_3)$	1.4×10^{-5}
$[Pt(bpy)(C_8H_4S_8)](I_3)_{0.9}$	1.3×10^{-3}
$[Pt(bpy)(C10\text{-}C_6S_8)](I_3)$	6.8×10^{-5}
$[Pt(Bu\text{-}pya)(C_8H_4S_8)](TCNQ)_{0.6}$	6.6×10^{-5}
$[Pt(bpy)(C_8H_4S_8)](TCNQ)_{0.8}$	6.5×10^{-3}
$[Pt(bpy)(C10\text{-}C_6S_8)](TCNQ)_{0.6}$	5.6×10^{-5}
$[Pt(bpy)(C_8H_4S_8)][BF_4]$ [b]	4.0×10^{-3}
$[Pt(bpy)(C_3S_5)](I_3)_{0.7}$ [c]	4.1×10^{-8}
$[Pt(Et\text{-}pya)(C_3S_5)](I_3)_{0.6}$ [c]	1.3×10^{-6}

[a] Measured for compacted pellets at r.t.

[b] By electrolysis.

[c] Ref. [29].

Planar $C_8H_4S_8$–metal complexes having another ligand and their oxidized species are expected to form new molecular associations. Planar complexes of the $[MN_2S_2]$-type containing both a diimine ligand as a π-electron acceptor and a dithiolate ligand as an electron donor are polarized around the metal ion in the ground state, exhibiting intramolecular mixed metal/ligand-to-ligand charge transfer (CT) band [21,22]. They may form molecular associations through interligand electrostatic interactions and/or metal–metal contacts, which are suitable for electron conduction. Partially oxidized and reduced square-planar platinum(II) complexes often form one-dimensional columnar structures through Pt···Pt interactions, showing high electrical conductivities [23,24]. Thus, polarized platinum(II) complexes having the $C_8H_4S_8$ and related sulfur-rich dithiolate ligands are likely to afford unique columnar and/or layered arrangements of complex molecules in the solid state, leading to new electrical conductors.

$[M(L)(C_8H_4S_8)]$ [M = Pd(II) and Pt(II); L = 2,2′-bipyridine (bpy), *N*-butyl- (Bu-pya) and *N*-decyl-pyridine-2-carbaldimine (C_{10}-pya)] were prepared [25,26]. These complexes showed an intense electronic absorption band at 680–810 nm due to the mixed metal/ligand-to-ligand CT transition, the band maxima being sensitive to solvent polarity. $[Pt(L)(C_8H_4S_8)]$ exhibited first oxidation potentials at -0.11 to -0.075 V (vs. Ag/Ag^+). They were reacted with excess amounts of iodine or 7,7,8,8-tetracyano-*p*-quinodimethane (TCNQ) to give the oxidized species as listed in Table 1. Current-controlled electrolysis of a CH_2Cl_2 solution of $[Pt(bpy)(C_8H_4S_8)]$ in the presence of $[NBu_4][BF_4]$ afforded needles of a one-electron oxidized species $[Pt(bpy)(C_8H_4S_8)][BF_4]$ (**3**) [27]. The crystal structure of **3** is shown in Fig. 1. The oxidized moieties are arranged in the same molecular direction to form a column along the *c* axis through some S···S non-bonded contacts. Furthermore, along the *b* axis there are some S···S contacts among the columns arranged in alternate molecular directions, resulting in a two-dimensional molecular interaction. The electron-conduction pathway is constructed along the *c* axis, which was deduced from band energy calculation. The electrical conductivities of the oxidized complexes were 5.6×10^{-5}–6.5×10^{-3} $S\,cm^{-1}$ measured for compacted pellets at r.t. (Table 1). They have an effective electron-conduction pathway through S···S contacts, as observed for the crystal structure of **3**, although the complexes having long *N*-alkyl groups exhibit somewhat low electrical

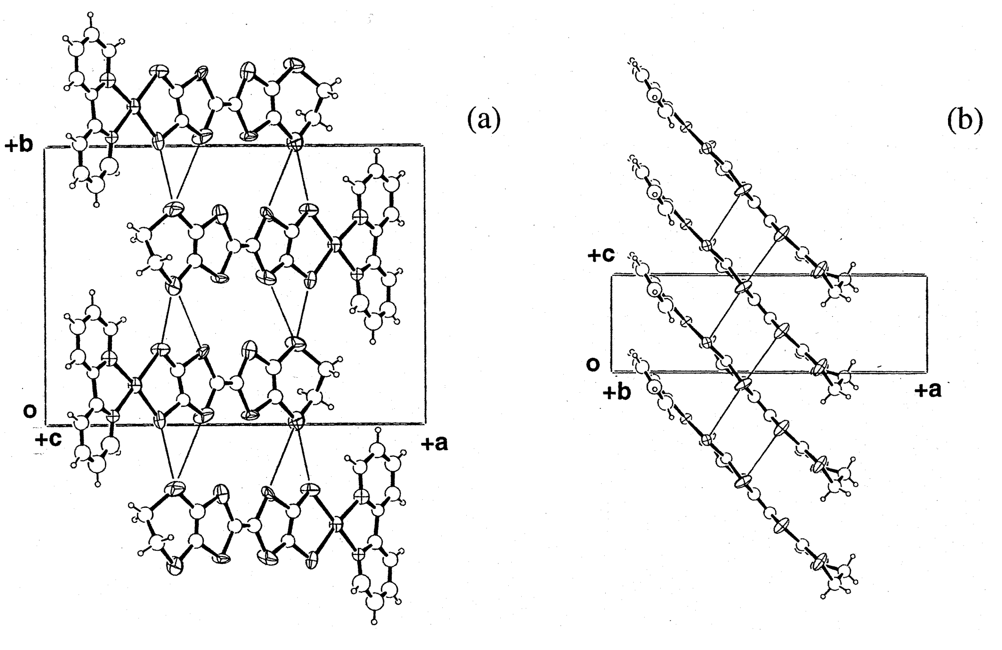

Fig. 1. Perspective views of the packing of cation moieties of **6** along the *b* axis (a) and the *c* axis (b). Fine lines indicate S···S non-bonded contacts (< 3.7 Å) [27].

conductivities. The one-electron oxidized complex $[NBu_4][Ni(CN)_2(C_8H_4S_8)]$ of the planar $[MC_2S_2]$-type was prepared and the crystal structure clarified [28]. However, it is an insulator, since it forms a dimer with short S···S non-bonded contacts in the solid state. The related oxidized C_3S_5–Pt(II) complexes $[Pt(L)(C_3S_5)]$-$(I_3)_x$ (L = bpy and *N*-ethyl-pyridine-2-carbaldimine; $x = 0.6$ and 0.7) exhibited low electrical conductivities [29].

Planar platinum(II) complexes with the $R_2C_6S_8^{2-}$ ligand (**B**) having long alkyl chains ($R = C_{10}H_{21}$, $C_{14}H_{29}$ and $C_{18}H_{39}$), $[NBu_4]_2[Pt(C_6S_8R_2)_2]$, were prepared (Scheme 1). These sulfur-rich dithiolate complexes are expected to have a layered structure as an organic–inorganic molecular composite with associations among long alkyl chains and among the sulfur-rich dithiolato–metal complex moieties. The crystal structure of $[NBu_4]_2[Pt\{C_6S_8(C_{10}H_{21})_2\}_2]$ (**4**) is shown in Fig. 2. The anion moieties are arranged through association of the long alkyl chains to form a layered structure. There are no significant interactions between the bis(dithiolato)platinum(II) center units owing to the presence of the bulky NBu_4^+ ion. For the oxidized species, however, some S···S interactions may occur between the bis(dithiolato)Pt(II) moieties in the absence of the bulky cations. These complexes have low oxidation potentials: $R = C_{10}H_{21}$, + 0.05 and + 0.38 V; $R = C_{14}H_{29}$, − 0.25 and + 0.25 V; $R = C_{18}H_{39}$, − 0.25 and + 0.05 V (vs. SCE). Fig. 3 shows electronic absorption spectra of **4** in CH_2Cl_2 in the presence of varying amounts of $[Fe(\eta^5\text{-}C_5H_5)_2][PF_6]$ as an oxidizing agent. The band at 1500 nm for **4** is ascribed to the dithiolate ligand-to-Pt(II) ion CT transition. With increase of the amount of the oxidized species, the band diminishes in intensity, accompanied with an increased intensity of the band at 1100 nm. These complexes react with $[Fe(\eta^5\text{-}C_5H_5)_2][PF_6]$, bromine or iodine to essentially afford

$$R_2C_6S_8(CH_2CH_2CO_2Et)_2 \xrightarrow[EtOH]{Na} Na_2[C_6S_8R_2] \xrightarrow[EtOH]{[NBu_4]_2[PtCl_4]}$$

$$[NBu_4]_2[Pt(C_6S_8R_2)_2] \quad (R = C_{10}H_{21}, C_{14}H_{29} \text{ and } C_{18}H_{39})$$

Scheme 1.

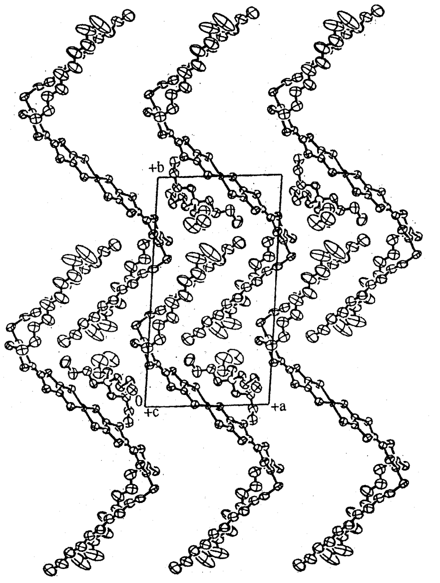

Fig. 2. Packing diagram of **4** [30].

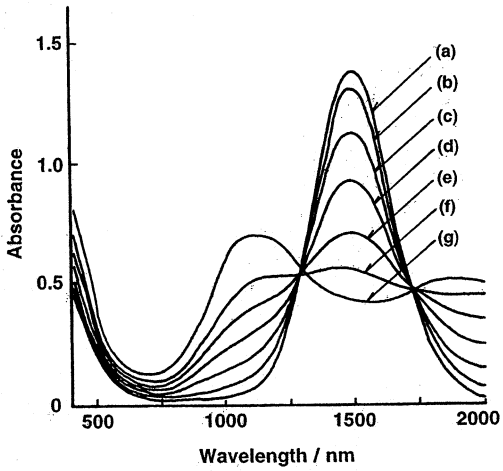

Fig. 3. Electronic absorption spectra of **4** (6.0×10^{-5} mol dm^{-3}) in CH_2Cl_2 in the presence of varying amounts of $[Fe(\eta^5\text{-}C_5H_5)_2][PF_6]$; (a) 0 to (g) 1.2×10^{-4} mol dm^{-3} [30].

two-electron oxidized species $[Pt(C_6S_8R_2)_2]^0$. Their electrical conductivities measured for compacted pellets at r.t. are: $R = C_{10}H_{21}$, 4.9×10^{-2}; $R = C_{14}H_{29}$, 2.5×10^{-2}; $R = C_{18}H_{39}$, $< 10^{-8}$ S cm^{-1}. The oxidation of these complexes results in effective packing of the $[Pt(C_6S_8)_2]$ units suitable for the formation of an electron-conduction pathway in the solid state, although the oxidized species with $R = C_{18}H_{39}$ is an insulator.

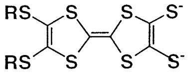

B

Additionally, some cobalt(III) complexes were also studied. $[NEt_4][Co\{C_6S_8(C_{10}H_{21})_2\}_2]$ (**5**) was obtained by a reaction of $[Co(acac)_3]$ (acacH = acetylacetone) with $Na_2[C_6S_8(C_{10}H_{21})_2]$ and $[NEt_4]Br$. The oxidized species obtained by the reaction with iodine, $[Co\{C_6S_8(C_{10}H_{21})_2\}_2]^0$ and $[Co\{C_6S_8(C_{10}H_{21})_2\}_2](I_3)_{0.7}$, exhibited electrical conductivities of 4.2×10^{-6} and 1.1×10^{-5} S cm^{-1} (compacted pellets at r.t.), respectively [31]. The Co(III)-anion moiety of **5** is likely to assume a square-pyramid geometry having a Co–S coordination from another anion and to form a dimeric structure in the solid state, as observed for some Co(III)–dithiolate complexes [32,33]. Association of the dithiolate moieties having long alkyl chains is ineffective for the formation of electron-conduction pathway. On the other hand, $[NEt_4][Co(C_8H_4S_8)_2]$ obtained by a reaction of $[Co(acac)_3]$ with $Na_2[C_8H_4S_8]$ and $[NEt_4]Br$ was oxidized to afford $[NEt_4]_{0.3}[Co(C_8H_4S_8)_2]$, exhibiting high electrical conductivity of 1.1×10^{-2} S cm^{-1} (compacted pellet at r.t.).

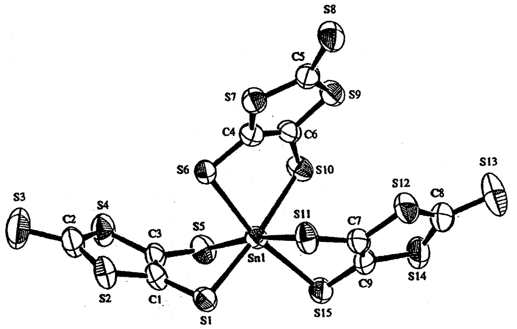

Fig. 4. Geometry of the anion of **6** [34].

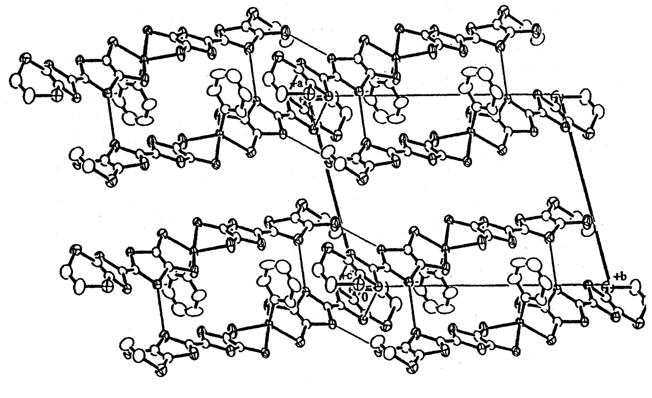

Fig. 5. Packing diagram of the anions of **8**. Fine lines indicate S···S contacts (< 3.7 Å) [34].

3. Bulky, hexa- and penta-coordinate metal complexes

Bulky, hexa-coordinate tin(IV) complexes with sulfur-rich dithiolate ligands, $[NMe_4]_2[Sn(C_3S_5)_3]$ (**6**), $[NEt_4]_2[Sn(C_8H_4S_8)_3]$ (**7**) and $[NBu_4][PhSn(C_8H_4S_8)_2]$ (**8**) were prepared by reactions of $SnCl_4 \cdot 2H_2O$ or $PhSnCl_3$ with $Na_2[C_3S_5]$ or $Na_2[C_8H_4S_8]$ [34]. The X-ray crystal structure analysis of **6** revealed a nearly octahedral geometry around the Sn(IV) atom (interligand transoid S–Sn–S angle, 170.80 (average)), as shown in Fig. 4. geometry is rather similar to those of [*N*-methylphenazinium]$_2[V(C_3S_5)_3]$ [transoid S–V–S angle, 161.8° (average)] [35] and of $[Fe(\eta^5\text{-}C_5Me_5)_2][W(C_3S_5)_3]$ [transoid S–W–S angle, 135.8° (average)] [36], and different from those of $[NBu_4]_2[M(C_3S_5)_3]$ [transoid S–M–S angle, M = Mo(IV), 146.5° and M = W(IV), 147.2° (average)] [36]. The crystal structure of **6** having the small cation moieties consists of some S···S non-bonded contacts (< 3.7 Å) among the anions. Complex **8** contains a penta-coordinate anion having an essentially trigonal bipyramidal geometry around the Sn(IV) atom connected with carbon and four sulfur atoms. The anion moieties form dimeric units which further interact with each other through S···S contacts, resulting in a one-dimensional array in the solid state (Fig. 5) [34]. The geometry of the anion is in contrast to those between rectangular square-pyramidal and trigonal bipyramidal of the $[RSn(C_3S_5)_2]^-$ anions (R = Bu and Ph [37]; $CH_2CH_2CO_2Me$ [38]).

Complex **6** exhibited an irreversible redox wave having oxidation peaks at + 0.24 and + 0.48 V (vs. Ag/Ag^+) in CH_2Cl_2. On the other hand, **7** showed pseudo-reversible oxidation peaks at − 0.26 and + 0.41 V in CH_2Cl_2. A cyclic voltammogram of **8** measured in DMF showed an irreversible wave having oxidation peak potentials at − 0.09 and + 0.08 V (vs. Ag/Ag^+). Complex **6** was oxidized by iodine or TCNQ to give C_6S_{10}. This compound is a C_3S_5-dimer, which was clarified by X-ray crystal structure analysis [34]. Although the molecular geometry is essentially identical to that of $C_6S_{10} \cdot 0.5CS_2$ reported previously [39], the molecules are closely packed through many S···S non-bonded contacts in the solid state. Complex **8** was also decomposed by the reaction with TCNQ in DMF to afford solids of $(C_8H_4S_8)_n$. On the other hand, oxidation reactions of **7** with TCNQ or iodine yielded essentially two-electron oxidized species $[Sn(C_8H_4S_8)_3]$ (**9**). This oxidized species exhibited electrical conductivity of 0.032 S cm^{-1} for a compacted pellet at r.t. Powders of **9** showed an isotropic EPR signal at $g = 2.008$, which is due to a small amount of paramagnetic one-electron oxidized species, indicating the $C_8H_4S_8$ ligand-centered oxidation. The powder reflectance spectrum of **9** showed broad bands at a longer wavelength region (Fig. 6), suggesting a molecular interaction between $C_8H_4S_8$ ligand moieties through S···S contacts. This interaction is likely to construct an effective electron-conduction pathway even in the bulky metal complex, leading to the high electrical conductivity. This is also the same for the oxidized $[M(C_3S_5)_3]$ species (M = Mo(IV), W(IV) [36] and Re(V) [40]).

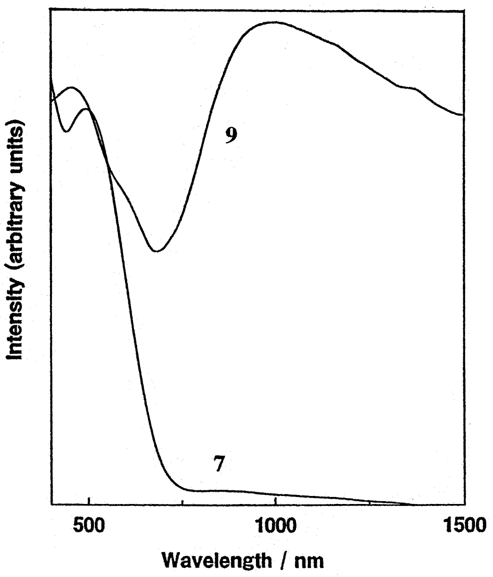

Fig. 6. Powder reflectance spectra of **7** and **9** [34].

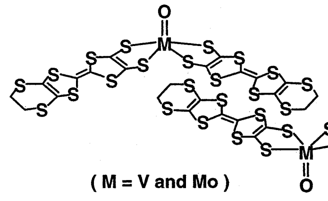

Fig. 7. A possible molecular array of the oxidized $[M(O)(C_8H_4S_8)_2]$ moieties with some S···S non-bonded contacts [41].

Penta-coordinate oxometallate complexes with sulfur-rich dithiolate ligands, $[NEt_4]_2[V(O)(C_8H_4S_8)_2]$ (**10**), $[NEt_4]_2[Mo(O)(C_8H_4S_8)_2]$ (**11**) were prepared by reactions of $[V(O)(acac)_2]$ or $[pyridinium]_2[Mo(O)Cl_5]$ with $Na_2[C_8H_4S_8]$ [41]. These complexes exhibited low oxidation potentials: − 0.21, + 0.14 V for **10** and − 0.18, + 0.04 V (vs. SCE) for **11**. These values are appreciably lower than those of corresponding $[M(O)(C_3S_5)_2]^{2-}$ complexes: M = V(IV), + 0.19 V [35] and M = Mo(IV), + 0.15 V (vs. SCE) [42]. Their oxidized species obtained from the oxidation by iodine or $[Fe(\eta^5\text{-}C_5Me_5)_2][BF_4]$, $[V(O)(C_8H_4S_8)_2]$ (**12**), $[NEt_4]_{0.3}[Mo(O)(C_8H_4S_8)_2]$ (**13**) and $[Fe(\eta^5\text{-}C_5Me_5)_2]_{0.05}[Mo(O)(C_8H_4S_8)_2]$ (**14**), exhibited high electrical conductivities: 0.12, 0.29 and 5.9 S cm^{-1} (compacted pellets at r.t.), respectively. These high values are in contrast to the values of the oxidized species of the corresponding $[M(O)(C_3S_5)_2]^{2-}$ (M = V(IV) and Mo(IV)) complexes: especially, the conductivities of the Mo(IV)-species **13** and **14** are much higher than those (6.7×10^{-9}–7.3×10^{-3} S cm^{-1}) of the oxidized $[M(O)(C_3S_5)_2]^{n-}$ ($n < 1$) species [35,42,43]. Such high electrical conductivities of the oxidized $[M(O)(C_8H_4S_8)_2]^{n-}$ (M = V(IV) and Mo(IV); $n < 1$) complexes come from effective molecular interaction through many S···S contacts in the solid state, as is seen in a possible molecular array (Fig. 7). This is based on a square-pyramidal geometry of the complexes, as observed for the structure of the $[Mo(O)(C_3S_5)_2]^{2-}$ complex [42].

4. Cyclopentadienyl–metal complexes

Organometallic complexes containing $C_3S_5^{2-}$ and $C_8H_4S_8^{2-}$ ligands are expected to become unique electrical conductors because of molecular inorganic–organic composites having columnar and/or layered structures constructed with S···S non-bonded interactions among the sulfur-rich dithiolate ligand moieties. Several C_3S_5–metal complexes containing cyclopentadienyl and pentamethylcyclopentadienyl groups have been studied as electroactive compounds [44–53]. However, no electrical conductors have been studied for these complexes. The oxidized species of the $C_8H_4S_8$–metal complexes are expected to form new packing structures with many S···S contacts in the solid state and to become good electrical conductors even in the metal complexes having non-planar geometries.

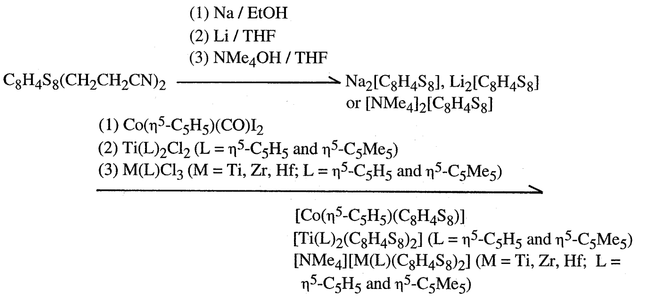

$$C_8H_4S_8(CH_2CH_2CN)_2 \xrightarrow[]{\text{(1) Na / EtOH; (2) Li / THF; (3) NMe}_4\text{OH / THF}} Na_2[C_8H_4S_8],\ Li_2[C_8H_4S_8] \text{ or } [NMe_4]_2[C_8H_4S_8]$$

$$\xrightarrow{\text{(1) Co}(\eta^5\text{-}C_5H_5)(CO)I_2;\ \text{(2) Ti(L)}_2Cl_2\ (L = \eta^5\text{-}C_5H_5 \text{ and } \eta^5\text{-}C_5Me_5);\ \text{(3) M(L)Cl}_3\ (M = Ti, Zr, Hf;\ L = \eta^5\text{-}C_5H_5 \text{ and } \eta^5\text{-}C_5Me_5)}$$

$[Co(\eta^5\text{-}C_5H_5)(C_8H_4S_8)]$
$[Ti(L)_2(C_8H_4S_8)_2]$ ($L = \eta^5\text{-}C_5H_5$ and $\eta^5\text{-}C_5Me_5$)
$[NMe_4][M(L)(C_8H_4S_8)_2]$ (M = Ti, Zr, Hf; $L = \eta^5\text{-}C_5H_5$ and $\eta^5\text{-}C_5Me_5$)

Scheme 2.

Several η^5-C_5H_5– and η^5-C_5Me_5–metal complexes with the $C_8H_4S_8$ ligand were prepared according to Scheme 2 [54–57].

The geometry of $[Co(\eta^5\text{-}C_5H_5)(C_8H_4S_8)]$ (**15**) is presumably similar to that of $[Co(\eta^5\text{-}C_5H_5)(C_3S_5)]$ [53]. The crystal structure of $[Ti(\eta^5\text{-}C_5Me_5)_2(C_8H_4S_8)]$ (**16**) was clarified by X-ray analysis, the geometry being displayed in Fig. 8. The complex exhibits a characteristic folding of the TiS_2C_2 plane, which is very similar to the case of $[Ti(\eta^5\text{-}C_5Me_5)_2(C_3S_5)]$ [49]. In accordance with this finding, ^{1}H NMR spectra of $[Ti(\eta^5\text{-}C_5H_5)_2(C_8H_4S_8)]$ and **16** showed the non-equivalence of η^5-C_5H_5 and η^5-C_5Me_5 rings at low temperatures [55]. Geometries of $[M(L)(C_8H_4S_8)_2]^-$ (M = Ti(IV), Zr(IV) and Hf(IV); $L = \eta^5\text{-}C_5H_5$ and $\eta^5\text{-}C_5Me_5$) complexes are likely to be similar to those for $[Ti(L)(\text{dithiolate})_2]^-$ ($L = \eta^5\text{-}C_5H_5$ and $\eta^5\text{-}C_5Me_5$) complexes [47,58,59].

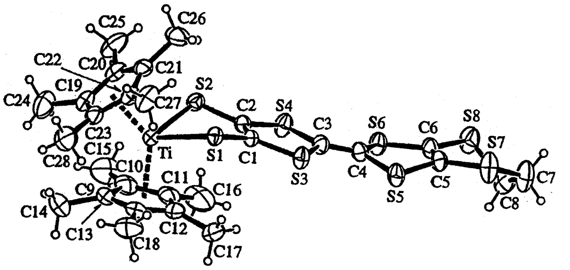

Fig. 8. Molecular geometry of **16** [55].

Table 2 summarizes reduction and oxidation peak potentials of the complexes. Complex **15** is reduced at −0.63 V (vs. SCE) in DMF, which is ascribed to Co(III) to Co(II) [54]. $[Ti(\eta^5\text{-}C_5H_5)_2(C_8H_4S_8)]$ and **16** are reduced at −1.40 and −1.63 V (vs. Ag/Ag$^+$), which are due to the Ti(IV) to Ti(III) process [55], while the Zr(IV)–$C_8H_4S_8$ complexes exhibited no reduction waves in this region [57]. The oxidation of the $C_8H_4S_8$ ligand of these neutral η^5-C_5H_5– and η^5-C_5Me_5–metal complexes occurs at low potentials of +0.11 to +0.29 V (vs. Ag/Ag$^+$). They are appreciably lower than those of the corresponding C_3S_5–metal complexes [45,49]. Anionic $[M(L)(C_8H_4S_8)_2]^-$ (M = Ti(IV), Zr(IV) and Hf(IV); $L = \eta^5\text{-}C_5H_5$ and $\eta^5\text{-}C_5Me_5$) complexes exhibited extremely low oxidation potentials (−0.39 to −0.20 V vs. Ag/Ag$^+$), as listed in Table 2. These findings are similar to the cases of $[Pt(C_8H_4S_8)_2]^{2-}$ (−0.48 V vs. SCE) [14] and $[M(O)(C_8H_4S_8)_2]^{2-}$ (M = V(IV) and Mo(IV)) complexes (−0.21 and −0.18 V vs. SCE) [41].

Complexes **15** and **16** and the other neutral Ti(IV)- and Zr(IV)-complexes were oxidized by iodine or $[Fe(\eta^5\text{-}C_5H_5)_2](PF_6)$ to give essentially one-electron oxidized species listed in Table 3. Anionic $[M(L)(C_8H_4S_8)_2]^-$ (M = Ti(IV), Zr(IV) and Hf(IV); $L = \eta^5\text{-}C_5H_5$ and $\eta^5\text{-}C_5Me_5$) complexes having lower oxidation potentials were oxidized by iodine or TCNQ to afford 1.3 and 1.8-electron oxidized complexes (Table 3). The oxidized species contain the I_3^- ion or the TCNQ$^{\bullet -}$ radical anion as a counter anion, which were confirmed by Raman and IR spectra [54,55,57]. The one-electron oxidized complex $[Co(\eta^5\text{-}C_5H_5)(C_8H_4S_8)](I_3)$ is compared with the oxidized species $[CoBr(\eta^5\text{-}C_5Me_5)(C_3S_5)]$ [60]. Since $[Co(\eta^5\text{-}C_5Me_5)(C_3S_5)]$ exhibits an oxidation potential of 0.388 V (vs. Ag/Ag$^+$) [45], it was not oxidized by iodine, but oxidized by bromine to afford the complex having the Co–Br bond. This oxidized species has the Co(III) ion and the one-electron oxidized C_3S_5 ligand, which was confirmed by EPR, XPS

Table 2
Reduction and oxidation peak potentials (V vs. Ag/Ag$^+$) and ΔE ($= E_{cp} - E_{ap}$, mV) in parentheses determined from cyclic voltammograms for the $C_8H_4S_8$–metal complexes [57]

Complex	Solvent	Peak potential		
		Reduction	Oxidation	
$[Co(\eta^5\text{-}C_5H_5)(C_8H_4S_8)]$ (**15**)	DMF	−0.85 (60)	+0.20 (65)	
$[Ti(\eta^5\text{-}C_5H_5)_2(C_8H_4S_8)]$	CH_2Cl_2	−1.40 (220)	+0.29 (210)	+0.73 (370)
$[Ti(\eta^5\text{-}C_5Me_5)_2(C_8H_4S_8)]$ (**16**)	CH_2Cl_2	−1.63 (280)	+0.19 (260)	+0.69 (340)
$[Zr(\eta^5\text{-}C_5H_5)_2(C_8H_4S_8)]$	CH_2Cl_2		+0.11	+0.76 (460)
$[NMe_4][Ti(\eta^5\text{-}C_5H_5)(C_8H_4S_8)_2]$	Acetone	−1.36 (80)	−0.39 (170)	
$[NMe_4][Ti(\eta^5\text{-}C_5Me_5)(C_8H_4S_8)_2]$	Acetone	−1.73 (320)	−0.20 (330)	+0.23 (330)
$[NMe_4][Zr(\eta^5\text{-}C_5H_5)(C_8H_4S_8)_2]$	CH_2Cl_2		−0.29 (160)	+0.64 (110)
$[NMe_4][Zr(\eta^5\text{-}C_5Me_5)(C_8H_4S_8)_2]$	CH_2Cl_2		−0.25 (200)	+0.19 (360)
$[NMe_4][Hf(\eta^5\text{-}C_5Me_5)(C_8H_4S_8)_2]$	CH_2Cl_2		−0.26 (180)	+0.09 (190)

Table 3
Electrical conductivities (σ)[a] of the oxidized η^5-C_5H_5– and η^5-C_5Me_5–metal complexes [54–57]

Complex	$\sigma_{r.t.}$ (S cm^{-1})
$[Co(\eta^5\text{-}C_5H_5)(C_8H_4S_8)](I_3)$	0.19
$[Co(\eta^5\text{-}C_5H_5)(C_8H_4S_8)](PF_6)_{0.7}$	0.16
$[Ti(\eta^5\text{-}C_5H_5)_2(C_8H_4S_8)](I_3)$	8.9×10^{-4}
$[Ti(\eta^5\text{-}C_5H_5)_2(C_8H_4S_8)](PF_6)$	2.9×10^{-3}
$[Ti(\eta^5\text{-}C_5Me_5)_2(C_8H_4S_8)](I_3)$	9.9×10^{-4}
$[Ti(\eta^5\text{-}C_5Me_5)_2(C_8H_4S_8)](PF_6)$	3.0×10^{-4}
$[Zr(\eta^5\text{-}C_5H_5)_2(C_8H_4S_8)](I_3)$	0.11
$[Ti(\eta^5\text{-}C_5H_5)(C_8H_4S_8)_2](I_3)_{0.3}$	0.16
$[Ti(\eta^5\text{-}C_5H_5)(C_8H_4S_8)_2](TCNQ)_{0.3}$	0.12
$[Ti(\eta^5\text{-}C_5Me_5)(C_8H_4S_8)_2](I_3)_{0.8}$	7.6×10^{-4}
$[Ti(\eta^5\text{-}C_5Me_5)(C_8H_4S_8)_2](TCNQ)_{0.3}$	0.055
$[Zr(\eta^5\text{-}C_5H_5)(C_8H_4S_8)_2]$	1.0×10^{-4}
$[Zr(\eta^5\text{-}C_5Me_5)(C_8H_4S_8)_2](I_3)_{0.8}$	4.9×10^{-4}
$[Zr(\eta^5\text{-}C_5Me_5)(C_8H_4S_8)_2](TCNQ)_{0.3}$	0.040
$[Hf(\eta^5\text{-}C_5Me_5)(C_8H_4S_8)_2](I_3)_{0.83}$	1.9×10^{-4}
$[Hf(\eta^5\text{-}C_5Me_5)(C_8H_4S_8)_2](TCNQ)_{0.3}$	0.010

[a] Measured for compacted pellets at r.t.

spectra and by calculated spin densities [60]. These oxidized $C_8H_4S_8$ complexes show an intense, almost isotropic EPR signal at $g = 2.004$–2.01, which is assigned to the radical species of the oxidized $C_8H_4S_8$ ligand moiety, as observed for radicals of oxidized C_3S_5– [17,36,60] and $C_8H_4S_8$–metal complexes [13,41]. The $C_8H_4S_8$ ligand-centered oxidation was confirmed by the calculated spin densities of the $[Ti(\eta^5\text{-}C_5H_5)_2(C_8H_4S_8)]^{\bullet+}$ radical cation species. The calculated spin density-isosurface of the paramagnetic oxidized species is shown in Fig. 9 [57]. Mulliken spin densities for this oxidized complex evaluated by a DFT calculation show the presence of about 85% spins on the $C_8H_4S_8$ ligand: Ti, 0.156; S(1), −0.003; S(2), 0.003; S(3), 0.153; S(4), 0.149; S(5), 0.119; S(6), 0.129; S(7), 0.014; S(8), 0.007; C(1), 0.057; C(2), 0.053; C(3), 0.032; C(4), 0.109; C(5), 0.020; C(6), 0.028. This observation is similar to the presence of 90% spins on the C_3S_5 ligand of the one-electron oxidized species $[CoBr(\eta^5\text{-}C_5Me_5)(C_3S_5)]$ [60].

Electrical conductivities of the oxidized complexes measured for compacted pellets at r.t. are listed in Table 3. All the complexes behave as semiconductors. Conductivities of the Ti(IV) complexes having two η^5-C_5H_5 or two η^5-C_5Me_5 groups are not high. This may come from insufficient molecular packing of the complex moieties in the solid state, resulting in ineffective S···S non-bonded contacts among the $C_8H_4S_8$ ligands. However, it is noteworthy that $[Zr(\eta^5\text{-}C_5H_5)_2(C_8H_4S_8)](I_3)$ shows a high electrical conductivity of 0.11 S cm^{-1}, as observed for $[Co(\eta^5\text{-}C_5H_5)(C_8H_4S_8)](I_3)$ and $[Co(\eta^5\text{-}C_5H_5)(C_8H_4S_8)](PF_6)_{0.7}$. For the oxidized $[M(L)(C_8H_4S_8)_2]^{n+}$ (L = η^5-C_5H_5 and η^5-C_5Me_5; M = Ti(IV), Zr(IV) and Hf(IV); $n = 0$–0.8) complexes, the electrical conductivities of the 1.3-electron oxidized species ($n = 0.3$) are appreciably high compared with the other oxidized complexes ($n = 0$ and 0.8). This partially oxidized state ($n = 0.3$) of the complex moiety seems to be more suitable for the electron-conduction through the packed complex moieties in the solid state. Particularly $[Ti(\eta^5\text{-}C_5H_5)(C_8H_4S_8)_2]^{0.3+}$ complexes having a less bulky η^5-C_5H_5 group exhibit high conductivities. The non-planar geometry around the metal ion for these species is somewhat similar to those of penta-coordinate $[M(O)(C_8H_4S_8)_2]$ [M = V(IV) and Mo(IV)] complexes [41]. Even in the bulky geometries of the 1.3-electron oxidized complexes good electron-conduction pathways are likely to be constructed by S···S contacts in the solid state.

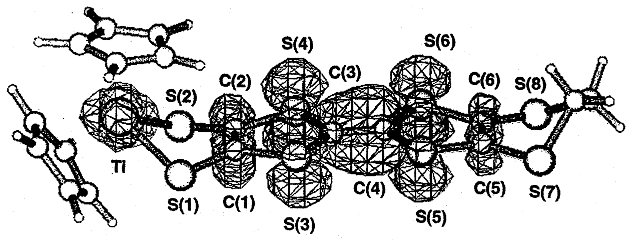

Fig. 9. Spin density-isosurface (0.001 e Å^{-3}) of the $[Ti(\eta^5\text{-}C_5H_5)_2(C_8H_4S_8)]^{\bullet+}$ radical cation species evaluated by a DFT calculation [41].

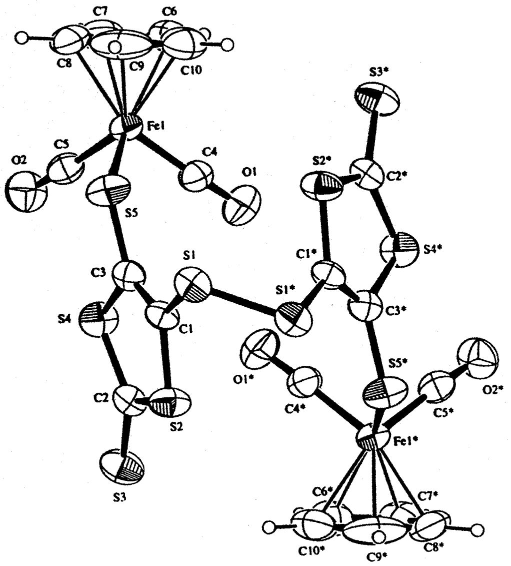

Fig. 10. Molecular geometry of **17** [61].

Reactions of $[Fe(\eta^5\text{-}C_5H_5)(CO)_2I]$ with Na_2L (L = $C_3S_5^{2-}$ and $C_8H_4S_8^{2-}$) in EtOH, followed by air-oxidation, afforded $[Fe(\eta^5\text{-}C_5H_5)(CO)_2(L\text{–}L)Fe(\eta^5\text{-}C_5H_5)(CO)_2]$ (L–L = C_3S_5–C_3S_5 (**17**) and $C_8H_4S_8$–$C_8H_4S_8$ (**18**)) [61]. These complexes with the S–S coupled, dimerized dithiolate ligands (L–L) were confirmed by electrospray mass spectra, molecular weight and by the X-ray crystal analysis for **17** (Fig. 10). This complex contains the S–S coupled $C_6S_{10}^{2-}$ dianion. The dianion salt, $[NMe_4]_2[C_6S_{10}]$, was recently prepared and the molecular structure clarified, together with that of the related dianion salt $[PPh_4]_2[C_{12}S_{16}]$ [62]. The oxidation of **17** proceeded by the reaction with bromine, followed by the cleavage of the Fe–S bond, to give $(C_3S_5)_2$ [34], which was confirmed by IR spectra. On the other hand, the reaction of **18** with excess amount of iodine afforded black solids of the oxidized species $[Fe(\eta^5\text{-}C_5H_5)(CO)_2(C_8H_4S_8\text{–}C_8H_4S_8)Fe(\eta^5\text{-}C_5H_5)(CO)_2](I_{10.5})$. This species contains both the I_3^- and I_5^- ions as the counter ion, which was confirmed by Raman spectra. Thus, it is oxidized beyond two electrons, and contains the oxidized $(C_8H_4S_8)_2$ ligand and the Fe(III) state. This oxidized complex exhibited an electrical conductivity of 1.7×10^{-4} S cm^{-1} measured for a compacted pellet at r.t. This indicates a molecular interaction via S···S contacts among the $C_8H_4S_8$ moieties even for bulky oxidized species.

5. Conclusions

Various kinds of metal complexes having the $C_8H_4S_8$ ligand as a further extended π-electron system or related sulfur-rich dithiolate ligands were prepared. They have appreciable low oxidation potentials due to the oxidation of the sulfur-rich dithiolate ligands compared with those of the corresponding C_3S_5–metal complexes. Stable oxidized complexes were obtained by reactions with iodine, $[Fe(\eta^5\text{-}C_5H_5)_2]^+$, $[Fe(\eta^5\text{-}C_5Me_5)_2]^+$, or TCNQ or by electrolysis. They exhibited EPR signals ascribed to paramagnetic species due to the $C_8H_4S_8$ ligand-centered oxidation. Effective electron-conduction pathways were formed through many S···S nonbonded contacts among the oxidized $C_8H_4S_8$ ligand moieties in the solid state, resulting in high electrical conductivities even for non-planar, bulky metal complexes. Thus, oxidized $C_8H_4S_8$–metal complexes having various geometries can be assembled mainly through many S···S contacts in the solid state leading to interesting electrical and magnetic properties.

Acknowledgements

We are grateful to Professor S. Suzuki (Osaka University) for measurement of EPR spectra, to Professor R. Arakawa (Kansai University) for measurement of electrospray mass spectra and to Dr I. Kawafune (Osaka Municipal Institute of Technology) for measurement of X-ray photoelectron spectra. Our research was supported in part by Grant-in-aids for Scientific Research (Nos. 90640665, 09239231, 10133230, 11120228, 11136223 and 12023225) from Ministry of Education, Science, Sports and Culture, Japan.

References

[1] P. Cassoux, L. Valade, K. Kobayashi, A. Kobayashi, R.A. Clark, A.E. Underhill, Coord. Chem. Rev. 110 (1991) 115.

[2] G. Matsubayashi, Rev. Heteroatom Chem. 4 (1991) 171.

[3] R.-M. Olk, B. Olk, W. Dietzsch, R. Kirmse, E. Hoyer, Coord. Chem. Rev. 117 (1992) 99.

[4] A.E. Pullen, R.-M. Olk, Coord. Chem. Rev. 188 (1999) 211.

[5] R. Kato, Y. Kashimura, S. Aonuma, N. Hanasaki, H. Tajima, Solid State Commun. 105 (1998) 561.

[6] N.L. Narvor, N. Robertson, E. Wallace, J.D. Kilburn, A.E. Underhill, P.N. Bartlett, M. Webster, J. Chem. Soc. Dalton Trans. (1996) 823.

[7] N.L. Narvor, N. Robertson, T. Weyland, J.D. Kilburn, A.E. Underhill, M. Webster, N. Svenstrup, J. Becher, Chem. Commun. (Cambridge) (1996) 1363.

[8] M. Kumasaki, H. Tanaka, A. Kobayashi, J. Mater. Chem. 8 (1998) 295.

[9] K. Ueda, M. Goto, M. Iwamatsu, T. Sugimoto, S. Endo, N. Toyota, K. Yamamoto, H. Fujita, J. Mater. Chem. 8 (1998) 2195.

[10] A. Kobayashi, M. Kumasaki, H. Tanaka, Synth. Met. (1999) 1768.

[11] A. Kobayashi, H. Tanaka, M. Kumasaki, H. Torii, B. Narymbetov, T. Adachi, J. Am. Chem. Soc. 121 (1999) 10763.

[12] H. Tanaka, Y. Okano, H. Kobayashi, W. Suzuki, A. Kobayashi, Science 291 (2001) 285.

[13] M. Nakano, A. Kuroda, G. Matsubayashi, Inorg. Chim. Acta 254 (1997) 189.

[14] M. Nakano, A. Kuroda, H. Tamura, R. Arakawa, G. Matsubayashi, Inorg. Chim. Acta 279 (1998) 165.

[15] N. Svenstrup, K.M. Rasmussen, T.K. Kansen, J. Becher, Synthesis (1994) 809.

[16] L. Binet, J.M. Fabre, C. Montginoul, K.B. Simonsen, J. Becher, J. Chem. Soc. Perkin Trans. 1 (1996) 783.

[17] G. Matsubayashi, A. Yokozawa, J. Chem. Soc. Dalton Trans. (1990) 3535.

[18] Y. Sakamoto, G. Matsubayashi, T. Tanaka, Inorg. Chim. Acta 113 (1986) 137.

[19] M. Nakano, A. Kuroda, T. Maikawa, G. Matsubayashi, Mol. Cryst. Liq. Cryst. 284 (1996) 301.

[20] A.J. Schultz, H.H. Wang, L.C. Sonderholm, T.L. Sifter, J.M. Williams, K. Bechgaard, M.-H. Whangbo, Inorg. Chem. 26 (1987) 3757.

[21] S.D. Cummings, R. Eisenberg, J. Am. Chem. Soc. 118 (1996) 1949 (and references therein).

[22] C.-T. Chen, S.-Y. Liao, K.-J. Lin, C.-H. Chen, T.-Y.J. Lin, Inorg. Chem. 38 (1999) 2734.

[23] J.S. Miller (Ed.), Extended Linear Chain Compounds, vol. 3, Plenum, New York, 1983.

[24] R. Palmans, D.B. MacQueen, C.G. Pierpont, A.J. Frank, J. Am. Chem. Soc. 118 (1996) 12647.

[25] A. Nakahama, M. Nakano, G. Matsubayashi, Inorg. Chim. Acta 184 (1999) 55.

[26] K. Kubo, M. Nakano, H. Tamura, G. Matsubayashi, Inorg. Chim. Acta 311 (2000) 6.

[27] K. Kubo, M. Nakano, H. Tamura, G. Matsubayashi, Inorg. Chim. Acta (2001) submitted for publication.

[28] T. Naito, N. Kobayashi, T. Inabe, Chem. Lett. (1998) 723.

[29] G. Matsubayashi, M. Hirao, T. Tanaka, Inorg. Chim. Acta 144 (1988) 217.

[30] T. Nakazono, M. Nakano, H. Tamura, G. Matsubayashi, J. Mater. Chem. 9 (1999) 2413.

[31] K. Kubo, M. Nakano, G. Matsubayashi, submitted for publication.

[32] M.J. Baker-Hawkes, Z. Dori, R. Eisenberg, H.B. Gray, J. Am. Chem. Soc. 90 (1968) 4253.

[33] J.V. Rodorigues, I.C. Santos, V. Gama, R.T. Henrigues, J.C. Waerenborgh, M.T. Duarte, M. Almeida, J. Chem. Soc. Dalton Trans. (1994) 2655.

[34] T. Akasaka, M. Nakano, H. Tamura, G. Matsubayashi, submited for publication.

[35] G. Matsubayashi, K. Akiba, T. Tanaka, Inorg. Chem. 27 (1988) 4744.

[36] G. Matsubayashi, K. Douki, H. Tamura, M. Nakano, W. Mori, Inorg. Chem. 32 (1993) 5990.

[37] S.M.S.V. Doidge-Harrison, R.A. Howie, J.T.S. Irvine, G.M. Spencer, J.M. Wardell, J. Organomet. Chem. 436 (1992) 23.

[38] H. Buchanan, R.A. Howie, A. Khan, G.M. Spencer, J.L. Wardell, J.H. Aupers, J. Chem. Soc. Dalton Trans. (1996) 541.

[39] X. Yang, T.B. Rauchfuss, S. Wilson, J. Chem. Soc. Chem. Commun. (1990) 34.

[40] G. Matsubayashi, T. Maikawa, M. Nakano, J. Chem. Soc. Dalton Trans. (1993) 2995.

[41] G. Matsubayashi, M. Nakano, K. Saito, T. Yonamine, R. Arakawa, J. Organomet. Chem. 611 (2000) 364.

[42] G. Matsubayashi, T. Nojo, T. Tanaka, Inorg. Chim. Acta 154 (1988) 133.

[43] T. Nojo, G. Matsubayashi, T. Tanaka, Inorg. Chim. Acta 159 (1989) 49.

[44] X. Yang, T.B. Rauchfuss, S.R. Wilson, J. Am. Chem. Soc. 111 (1989) 3465.

[45] H. Ushijima, S. Sudoh, M. Kajitani, K. Shimizu, T. Akiyama, A. Sugimori, Inorg. Chim. Acta 175 (1990) 11.

[46] H. Ushijima, S. Sudoh, M. Kajitani, K. Shimizu, T. Akiyama, A. Sugimori, Appl. Organomet. Chem. 5 (1991) 221.

[47] F. Guyon, C. Lenoir, M. Fourmigue, J. Larsen, J. Amaudrut, Bull. Soc. Chim. Fr. 131 (1994) 217.

[48] F. Guyon, J. Amaudrut, M.-F. Mercier, K. Shimizu, J. Organomet. Chem. 465 (1994) 187.

[49] F. Guyon, M. Foumigue, P. Audebert, J. Amaudrut, Inorg. Chim. Acta 239 (1995) 117.

[50] M. Fourmigue, C. Lonoir, C. Coulon, F. Guyon, J. Amaudrut, Inorg. Chem. 34 (1995) 4979.

[51] S. Inomata, H. Takano, K. Hiyama, H. Tobita, H. Ogino, Organometallics 14 (1995) 2112.

[52] C. Faulmann, F. Delpech, I. Malfant, P. Cassoux, J. Chem. Soc. Dalton Trans. (1996) 2261.

[53] M. Fourmigue, V. Perrocheau, Acta Crystallogr. C 53 (1997) 1213.

[54] H. Mori, M. Nakano, H. Tamura, G. Matsubayashi, J. Organomet. Chem. 574 (1999) 77.

[55] K. Saito, M. Nakano, H. Tamura, G. Matsubayashi, Inorg. Chem. 39 (2000) 4815.

[56] G. Matsubayashi, M. Nakano, K. Saito, H. Tamura, Mol. Cryst. Liq. Cryst. 343 (2000) 29.

[57] K. Saito, M. Nakano, H. Tamura, G. Matsubayashi, J. Organomet. Chem. 625 (2001) 7.

[58] H. Kopf, K. Lange, J. Pickardt, J. Organomet. Chem. 420 (1991) 345.

[59] M.A. Spence, G.M. Rosair, W.E. Lindsell, J. Chem. Soc. Dalton Trans. (1998) 1581.

[60] H. Mori, M. Nakano, H. Tamura, G. Matsubayashi, W. Mori, Chem. Lett. (1998) 729.

[61] G. Matsubayashi, T. Ryowa, H. Tamura, M. Nakano, R. Arakawa, J. Organomet. Chem., in press.

[62] J.G. Breiter, A.I. Smirnov, L.F. Szczepura, S.R. Wilson, T.B. Rauchfuss, Inorg. Chem. 40 (2001) 1421.